Journal of Hydrology 549 (2017) 244–251

Contents lists available at ScienceDirect

Journal of Hydrology

journal homepage: www.elsevier.com/locate/jhydrol

Research papers

Runoff and soil loss characteristics on loess slopes covered with aeolian sand layers of different thicknesses under simulated rainfall

F.B. Zhang [a,b,*], Y.J. Bai [a], L.Y. Xie [a], M.Y. Yang [a,b], Z.B. Li [b,c], X.R. Wu [a]

[a] State Key Laboratory of Soil Erosion and Dryland Farming on the Loess Plateau, Institute of Soil and Water Conservation, Northwest A&F University, Yangling, Shaanxi Province 712100, PR China
[b] Institute of Soil and Water Conservation, CAS and MWR, Yangling, Shaanxi Province 712100, PR China
[c] State Key Laboratory Base of Eco-Hydraulic Engineering in Arid Area, Xi'an University of Technology, Xi'an, Shaanxi Province 710048, PR China

ARTICLE INFO

Article history:
Received 3 September 2016
Received in revised form 9 February 2017
Accepted 2 April 2017
Available online 4 April 2017

This manuscript was handled by Corrado Corradini, Editor-in-Chief, with the assistance of Nunzio Romano

Keywords:
Sediment yield
Runoff production
Runoff coefficient
Wind-Water Erosion Crisscross Region
Loess Plateau

ABSTRACT

In the Wind-Water Erosion Crisscross Region of the northern Loess Plateau, parts of loess slopes have been covered by layers of aeolian sand of different thicknesses. Knowledge of soil erosion processes and magnitudes on these slopes is essential to understanding the coupled water-wind erosion processes and to address the resulting downstream coarse sediment problems in the Yellow River. Simulated rainfall (intensity 90 mm h^{-1}) was performed to explore the effects of sand layer thickness on runoff and soil loss from loess slopes covered with different sand layer thicknesses (0, 0.5, 2, 5, 10, 15, 20, and 25 cm). Initial runoff time increased with increasing sand layer thickness, with greater changes occurring for the increases in the thinner (0–5 cm) than for the thicker layers (5–25 cm). Total runoff yield from the sand-covered loess slopes was 18%–55% lower than from the uncovered loess slope and decreased with increasing sand layer thickness. In contrast, total sediment yield was up to 14 times greater from the sand-covered loess slopes than from the uncovered loess slope and rapidly increased with increasing sand layer thickness. During the rainstorm, runoff and soil loss rates exhibited unimodal distributions, and they were related by a positive linear function, both before and after the maximum soil loss rate, that had a high determination coefficient ($R^2 > 0.8$, $p < 0.05$) on loess slopes with sand layer thicknesses greater than 5 cm. The maximum runoff and soil loss rates tended to occur simultaneously and increased abruptly with increasing sand layer thickness. During the rainstorms, some runoff rates on the loess slopes with thicker sand layers were higher than the rainfall intensity due to rainwater combining with water emerging from the saturated sand, which could never occur on the uncovered loess slope. The critical sand layer thickness, which produced a qualitative change in runoff and sediment production modes, appeared to be in the range of 5–10 cm. These results indicated that the thickness of the sand layer on the loess slope significantly influenced runoff and sediment production processes and mechanisms. These effects should be considered when assessing and predicting soil losses in this region and from similar slopes elsewhere.

1. Introduction

The Wind-Water Erosion Crisscross Region of the northern Loess Plateau undergoes the combined actions of water erosion in summer and autumn with wind erosion in winter and spring. It is an area of severe erosion with soil loss rates exceeding 10,000 t km^{-2} a^{-1} (Li et al., 2005). Previous studies in this region have indicated that the strong winds during the winter and spring transport large quantities of aeolian sand to the loess slopes, gullies and river channels. This results in a special geomorphologic landscape with layered soil profiles, i.e., the loess soil covered by layers of aeolian sand (Zhang et al., 1999; Xu et al., 2000), which are similar to texture-contrast or duplex soils (Rab et al., 1987; Tennant et al., 1992; Hardie et al., 2012a). Xu et al. (2000) estimated that the areas covered by this layered soil landscape total approximately 13,099 km^2 and are widely distributed in the Wind-Water Erosion Crisscross Region. The sand covering the loess can be easily eroded during subsequent rainy seasons and the eroded material then becomes a major source of the coarse sediment (>0.05 mm) that is transported by the Yellow River and deposited on the riverbeds of the Yellow River downstream (Xu, 2000, 2005b; Xu et al.,

* Corresponding author at: State Key Laboratory of Soil Erosion and Dryland Farming on the Loess Plateau, Institute of Soil and Water Conservation, Northwest A&F University, Yangling, Shaanxi Province 712100, PR China.
E-mail address: fbzhang@nwsuaf.edu.cn (F.B. Zhang).

http://dx.doi.org/10.1016/j.jhydrol.2017.04.002
0022-1694/

2000, 2006). Therefore, the problem of the great soil losses in this region is detrimental not only for the local agriculture and environment but also for the ecological sustainability of the lower reaches of the Yellow River (Xu et al., 2000; Wang et al., 2012; Zhou and Zhang, 2012).

In contrast to uniform soils, the layered soil profiles in the area of loess covered by aeolian sand have a clear boundary between the two layers (sand and loess) with very different chemical and physical properties, especially that of hydraulic conductivity (Wu et al., 2014). The low permeability of the subsoil is the factor that has the greatest influence on the behavior of these texture-contrast soils (Gregory et al., 1992; Tennant et al., 1992) and changes the responses to the infiltration and runoff modes on the slope (Gregory et al., 1992; Cox and McFarlane, 1995; Cox et al., 2002; Hardie et al., 2012a, 2013). A few studies have indicated that runoff and erosion processes on the sand-covered loess slopes are very different from those occurring on the uncovered loess slopes (Zhang et al., 1999; Xu et al., 2000, 2015). Zhang et al. (1999) performed two simulated rainfall experiments in the field and found that unique patterns of runoff and sediment production, i.e., infiltration-interflow-collapse processes, occurred on a sand-covered loess slope. Although runoff and sediment production were delayed, once runoff was initiated, the sediment yield rapidly increased with the runoff amount and was markedly higher on the sand-covered loess slopes than on the uncovered loess slopes. Zhang et al. (1999) also suggested that further studies were needed to explore the various effects of other factors that would affect the runoff and erosion processes and dynamic features on the sand-covered loess slopes under different conditions of rainfall, sand layer thickness, slope degree and slope length. Xu et al. (2015) conducted simulated rainfall experiments on sand-covered loess slopes in the laboratory and found that the thickness of the sand layer could affect runoff and sediment yield. However, the thickness of the covering sand layer considered in their study was too thin (less than 2 cm) to fully represent the runoff and erosion processes on the typical sand-covered loess slopes in the field. Even so, at the large scale, an analysis of data from the hydrometric stations led to the hypothesis that the hyperconcentrated flow occurring in the Wind-Water Erosion Crisscross Region and deposition of the coarser sediment particles on the riverbeds of the Yellow River downstream resulted because of the landscape of sand layers over loess (Xu, 2000, 2005a), and this hypothesis was supported by the findings of the limited laboratory studies.

Compared to the scarce studies of the sand-covered loess soils, more studies have been reported for the texture-contrast or duplex soils in other regions. The texture-contrast soils classified as "duplex" soils were definitively defined as having a subsoil (B horizon) with a texture that is at least one and a half texture groups finer than the surface soil (A Horizon), and the boundary between the surface soil and the subsoil has to be clear to sharp (Northcote, 1971). Physical and chemical characteristics of duplex soils, and the areas over which they were distributed across the Australian landmass have been determined (Rab et al., 1987; Chittleborough, 1992; Tennant et al., 1992). The large differences in the permeability of the subsoil and surface soil layers greatly affected the hydrological behavior of the duplex soils, and resulted in the formation of seasonal perched water tables, subsurface lateral flow, and numerous other management problems that were summarized by Hardie et al. (2013). Eastham et al. (2000) investigated water movement associated with a perched water-table in a duplex soil on a gentle (1.6%) slope and found that lateral water movement occurred in response to topographical gradients in the soil surface and the depth of the clay layer. The effects of antecedent soil water contents on hydraulic conductivity and preferential flow in duplex soils, and comparisons of subsurface lateral flow occurring in duplex soils with that in catchments with shallow bedrock have been studied in order to understand the mechanisms responsible for the development of perched water-tables and subsurface lateral flow in duplex soils (Hardie et al., 2011, 2012a,b, 2013). In addition, other studies considered seepage erosion and shallow landslides occurring on slopes with other kinds of texture-contrast soils worldwide to examine river bank failure (Fox et al., 2007; Karmaker and Dutta, 2013), embankment failure (Zeng et al., 2012; Raj and Sengupta, 2014), erosion of soil over bedrock (Hardie et al., 2012a; Lanni et al., 2013; Kim et al., 2015), and shallow landslides induced by rainfall (Okura et al., 2002; Wang and Sassa, 2003; Lourenço et al., 2006; Bogaard and Greco, 2016). However, while the sand covered loess soils can be described as texture-contrast or duplex soils, their characteristics differ from other kinds of texture-contrast soil due to their formation processes, the variations of layer thickness and the physico-chemical properties in their profiles. Although similar theories might possibly have been used to reveal infiltration, runoff and erosion/failure modes on other texture-contrast soil slopes, the characteristics of runoff and sediment production processes during rainstorms are expected to differ between them and the sand-covered loess slopes. Moreover, most studies of texture-contrast soil slopes mainly focused on variations in groundwater, water-table, pore pressure, seepage gradient forces, water content and other hydrological parameters in order to explain slope failure modes, mechanisms and processes. There are few studies that focused on variations in runoff and sediment production and their characteristics on texture-contrast soil slopes during rainstorms. Therefore, compared to the great progress made in understanding the processes of soil erosion on uniform soil slopes due to surface runoff and incorporating these in prediction technologies, the characteristics of the runoff and sediment production processes and mechanisms on the aeolian sand-covered loess slopes have not been completely identified and warrant further study.

The thickness of a coarser texture layer on a texture-contrast soil slope has been found to affect the infiltration mode, water-holding capacity and gravitational driving force (Kirkby and Chorley, 1967; Eastham et al., 2000; Okura et al., 2002; Chu and Mariño, 2005; Pornprommin et al., 2010) and subsequent runoff and sediment production patterns and processes (Xu et al., 2015). Variations in the depth of the sand layer covering the loess slopes in the Wind-Water Erosion Crisscross Region range from thin, in the order of millimeters, to thick, in the order of meters, due to the differences in the coupled interaction between wind and water erosion (Xu et al., 2000; Wu et al., 2014). However, no study of the effects of a wide range of sand layer thicknesses on runoff and erosion processes has been conducted for the sand-covered loess slopes. The objective of this paper is to analyze the influences of the thickness of an aeolian sand layer overlying a loess slope on hydrological and erosive processes during simulated rainfall. Our results are expected to provide insight into the runoff and sediment production from texture-contrast soil slopes and to enhance our understanding, prediction and control of soil losses in the Wind-Water Erosion Crisscross Region of the Loess Plateau.

2. Materials and methods

2.1. Experimental design

To achieve the objectives of this study, seven different thicknesses of an aeolian sand layer overlying a loess slope were established, i.e., 0.5, 2, 5, 10, 15, 20, and 25 cm thick, with uncovered soils (i.e., 0 cm thick) used as the control. The range of sand layer thicknesses investigated were based on field observations and on previous studies that simulated shallow landslides in the laboratory (Okura et al., 2002; Wang and Sassa, 2003; Lourenço et al.,

2006; Wu et al., 2014). The study was performed using simulated rainfall. A perforated metal flume (3 m in length, 1 m in width and 0.8 m in depth) for which the slope gradient could be adjusted from 0% to 70% was used to contain the soil. The depth from the base of the flume to the level of a collection funnel outlet at the lower end of the soil flume was 0.30 m, which ensured that the removal of soil by erosion did not unduly affect the erosion processes. Rainfall intensity (90 mm h^{-1}) and slope gradient (27%) were controlled factors in this study that were representative of the study area. A rainfall intensity of between 80 and 90 mm h^{-1} is typical of the intense storms in the semiarid regions of China that are dominated by monsoon climate conditions and contribute most to the annual soil losses on the Loess Plateau (Tang, 1990).

2.2. Soil flume preparation

The Liudaogou watershed, which is located in the Wind-Water Erosion Crisscross Region of the north Loess Plateau in Shenmu County, Shaanxi Province, is highly representative of the geomorphologic landscape of the sand-covered loess soils (Zhang et al., 1999). Accordingly, Lishi loess was collected from a steep profile in the Liudaogou watershed to use as subsoil, while aeolian sand was collected from a dune near the steep profile. The properties of the Lishi loess and aeolian sand are presented in Table 1. The Lishi loess was crushed to pass through a 4.0 mm sieve, which facilitated the removal of stones and debris while maintaining a reasonable quantity of aggregated soil, the water content was adjusted to approximately 10%, and the loess was then thoroughly mixed. The aeolian sand was air dried.

Two-layer profiles of aeolian sand overlying loess were created in the flume. First, the loess was packed uniformly into the flume in 5-cm thick layers to a total depth of 25 cm over a 5-cm layer of coarse sand used to facilitate drainage and/or to allow entrapped air to escape. The bulk density was approximately 1.45 mg m^{-3}, which was the representative of field measurements (Table 1). The surface of each sub-surface soil layer was gently scraped before packing the next layer to reduce discontinuities between layers. The top surface layer of loess was smoothed. The air-dried aeolian sand was added over the loess layer surface to give the intended thickness as indicated in Section 2.1. Finally the top surface of the aeolian sand layer was smoothed to reduce the influence of surface roughness. The toe of the aeolian sand layer adjacent to the funnel outlet was formed to create a slope of repose. The slope of prepared soil flume was adjusted to 27% for all of the rainfall simulation runs.

2.3. Rainfall application

Eight simulated rainstorms were conducted in the Simulated Soil Erosion Experiment Hall of the State Key Laboratory of Soil Erosion and Dryland Farming on the Loess Plateau, Institute of Soil and Water Conservation, CAS & MWR, Yangling. Simulated rainfall was produced from lateral jets at a height of 16 m above the ground. Raindrops (median diameter of 2.2 mm) followed a parabolic trajectory and fell vertically to the soil surface at close to the terminal velocity at a controllable intensity and with a distribution uniformity of over 85%. Tap water was used to simulate rainwater.

Although the rainfall intensity was set for 90 mm h^{-1}, the actual rainfall intensities measured by rain gauges for the eight runs were between 88.8 and 93 mm h^{-1}. Simulated rainfall was generally applied for more than 60 min for each run. During the simulated rainfall, a series of plastic containers with a volume of about 15 L were used sequentially to collect the entire runoff and sediment output from the soil flume, and the time between the changes of the containers was recorded in order to determine the sampling interval. The times of runoff initiation was also recorded. In addition, a series of photographs of the evolving surface erosion morphology were taken using a high-resolution camera mounted on a fixed ladder at a height of 3.5 m facing the soil flume. After each rainfall event, the runoff and sediment collected in each of the plastic containers were weighed and settled over 24 h. The sediment was subsequently recovered by settling, and the supernatant was removed from the water by siphoning. The settled sediment was weighed. A sample of the settled sediment was removed, weighed, oven dried at 105 °C and weighed again to calculate the sediment water content. The runoff amount and sediment yield could then be determined for each sampling interval.

3. Results

3.1. Runoff

Results presented in Table 2 show that the initial runoff time increased from 0.83 to 35.83 min as the thickness of the sand layer increased from 0 to 25 cm. However, the increases in the initial runoff time tended to be larger as the thickness increased from 0.5 to 5 cm and smaller for increases from 5 to 25 cm; in particular, the change in initial runoff time when the thickness increased from 15 to 25 cm was very small. During the 60 min of simulated rainfall, the total runoff yield from the uncovered loess slope was 18%–55% greater than the yields from the slopes with sand cover thicknesses of 0.5–25 cm. With an increase in the sand layer thickness from 0.5 to 25 cm, the total runoff yield decreased from 71.9 to 44.1 mm (Table 2). The decreasing trend was more intense in the range of thicknesses from 0.5 to 5 cm than in the range from 10 to 25 cm. Hence the total runoff yields in the 10 cm and 15 cm treatments were only slightly greater than the yield in the 5 cm treatment.

After runoff was initiated, the runoff rates during the simulated rainfall varied significantly with the change in sand layer thickness (Fig. 1). The runoff rates on the uncovered loess slope increased quickly during the 5 min after the incipient stage and then maintained a quasi-steady state. The runoff rates on the slopes with sand thicknesses of 0.5 cm and 2 cm increased fast after runoff initiation, followed by an almost steady stage with slight further increases. The runoff rates on the slope covered with 5 cm of sand increased sharply approximately 10 min after runoff initiation, reached a peak value, and then decreased slowly with fluctuations. For the runoff rates on the slopes covered with sand layers of

Table 1
Properties of the loessial soil and aeolian sand at the sampling site.

Soil type	Particle size content (%)			[a]BD (mg m^{-3})	P (%)	K_s (mm min^{-1})
	Sand (2–0.05 mm)	Silt (0.05–0.002 mm)	Clay (<0.002 mm)			
Aeolian sand	95.27 ± 3.06[b]	3.73 ± 1.70	1 ± 0.88	1.60 ± 0.04	39.6 ± 2.4	1.40 ± 0.46
Lishi loess	23.21 ± 2.09	66.63 ± 2.55	10.06 ± 0.47	1.43 ± 0.03	46.2 ± 1.4	0.05 ± 0.02

[a] BD, bulk density; P, porosity; Ks, saturated hydraulic conductivity.
[b] Data in the table are the mean ± one standard deviation.

Table 2
Eigenvalues of runoff and soil loss for each treatment during 60-min simulated rainstorms.

[a]hs (cm)	I (mm h^{-1})	IRT (min)	TR (mm)	$q_{r.max}$ (mm h^{-1})	RC_{max}	TM (kg m^{-2})	$q_{s.max}$ (kg m^{-2} h^{-1})
0	94.20	0.83	87.45	90.96	0.97	10.17	11.79
0.5	93.00	2.63	71.85	91.20	0.98	13.30	20.32
2	90.60	9.22	64.81	100.08	1.10	30.65	46.23
5	88.20	27.50	45.61	100.61	1.14	53.68	143.85
10	93.00	25.50	55.20	141.00	1.52	99.83	355.80
15	91.80	35.00	46.74	183.72	2.00	109.80	455.52
20	91.20	35.00	44.94	206.53	2.26	129.37	607.57
25	87.60	35.83	44.06	191.54	2.19	142.49	617.46

[a] hs, thickness of aeolian sand layer; I, rainfall intensity; IRT, initial runoff time; TR, total runoff; $q_{r.max}$, maximum runoff rate during the rainfall; RC_{max}, maximum runoff coefficient during the rainstorm; TM, total sediment yield; $q_{s.max}$, maximum soil loss rate during the rainstorm.

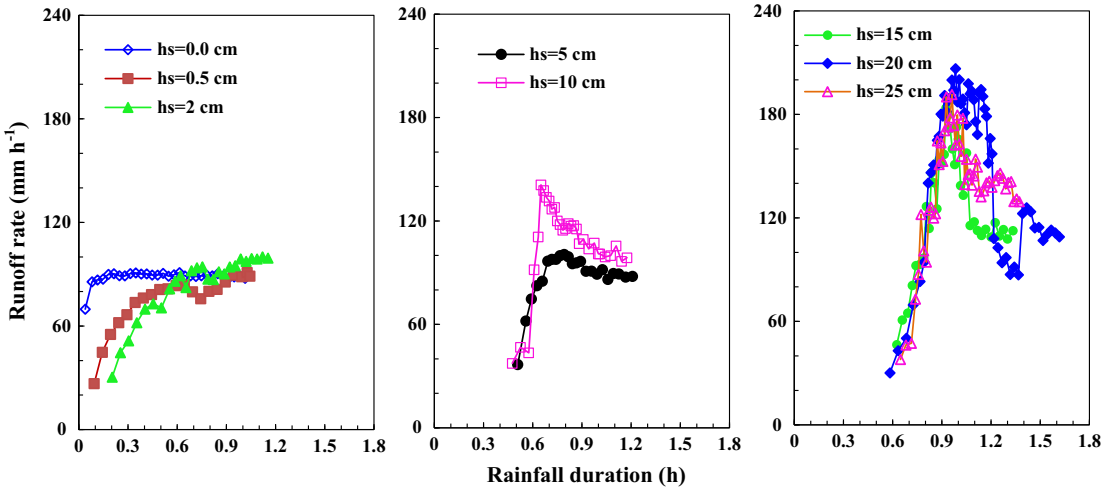

Fig. 1. Runoff rates on the loess slopes covered with aeolian sand layers of different thicknesses (hs) during simulated rainstorms.

10–25 cm, three distinct stages could be identified: a sharply increasing stage, a sharply decreasing stage, and a quasi-steady state stage. Some runoff rates during the rainfall were more than the actual rainfall intensity on the slopes with sand layer thicknesses greater than 2 cm. The maximum runoff rate during the rainfall among all treatments was 3.4 mm min^{-1} and was obtained from the slope with the 20 cm sand layer. In general, the maximum runoff rate for each treatment during the rainfall increased with the sand layer thickness (Table 2).

3.2. Soil loss

Fig. 2 presents the variation in the soil loss rate on the loess slopes with different sand layer thicknesses during the simulated rainstorms. The soil loss rate on the uncovered loess slope varied weakly throughout the rainstorm, although small initial increases followed by slight decreases after 27 min of rainfall are evident albeit with fluctuations. The variation in soil loss rates for both the 0.5 cm and 2 cm sand layer thicknesses during the rainstorms followed a similar pattern to that of the soil loss rates on the uncovered loess slope, but the soil loss rates and their variability were notably greater for the covered than for the uncovered loess slope. The variations in soil loss rates showed similar trends for the loess slopes under sand layers with thicknesses ranging from 5 to 25 cm; a fast increase, corresponding to the flushing out of sediments, and then a steep decrease that became relatively less steep until reaching a value approximately equal to the initial soil loss rate; this pattern was most clearly evident for the slope covered by the sand layer that was greater than 10 cm thick. The unimodal distribution of soil loss rates during the rainstorms became more evident with increasing sand layer thickness, and fluctuations in the soil loss rates were also more evident. The maximum soil loss rate and the range of soil loss rates occurring during the rainstorms tended to increase with the increasing thickness of the sand layer (Table 2).

The total sediment yield during 60 min of simulated rainfall increased from 13.3 to 142.5 kg m^{-2} as the thickness of the aeolian sand layer increased from 0.5 to 25 cm. A power expression with a power exponent of less than 1 and a determination coefficient of 0.99 related the total sediment yield produced during 60 min of simulated rainfall to the sand layer thickness (Table 2). The sediment yields on the sand-covered loess slopes were up to 14 times greater than that on the uncovered loess slope.

3.3. Relationship between runoff and soil loss

Under constant rainfall intensity and slope gradient, the relationship between total runoff and sediment yield during of rainfall was fitted by a negative power function for the different sand layer thicknesses. For the sand layer thicknesses of 0.5 and 2 cm, the changing patterns between the runoff and the soil loss rates during the rainstorm were similar to that observed for the uncovered loess slope, i.e., both rates generally increased during the early stage of the rainstorm but, in the later stage, the runoff rate entered a quasi-steady state and the soil loss rate gradually decreased (Figs. 1 and 2). For sand layer thicknesses greater than 5 cm, both soil loss and runoff rates exhibited similar patterns of change during the rainstorm and their relationships before and after the maximum soil loss rate was described by a positive linear function with a high correlation coefficient ($R^2 > 0.8$, $p < 0.05$) for

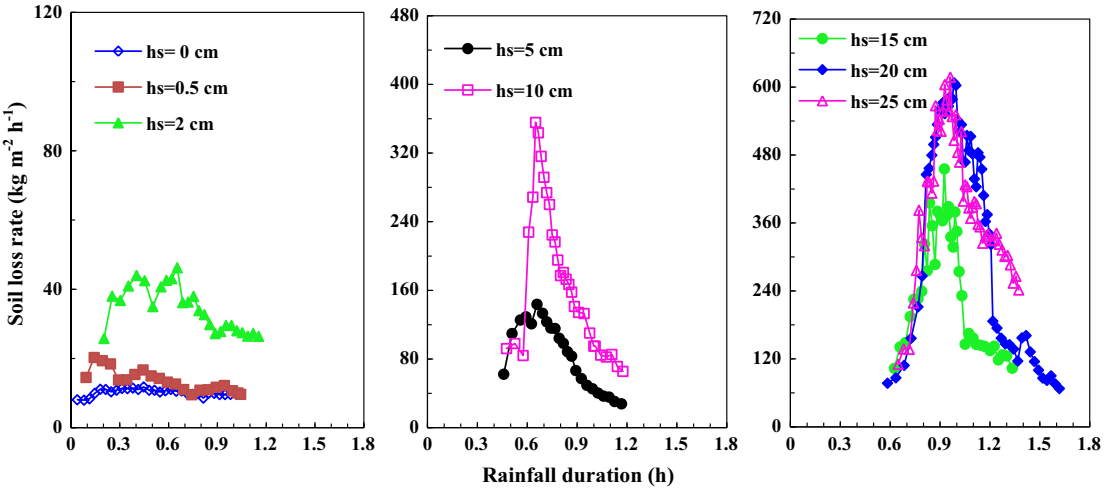

Fig. 2. Soil loss rates on the loess slopes covered with aeolian sand layers of different thicknesses (hs) during simulated rainstorms.

each treatment (Fig. 3). In addition, there was a significantly positive linear relationship between the maximum soil loss and runoff rates during the rainfall for the different treatments (Table 2), and they both appeared approximately simultaneously during the rainfall for sand layer thicknesses greater than 5 cm (Table 2 and Fig. 2).

4. Discussion

This study investigated the effects of sand layer thickness on runoff and sediment production on sand-covered loess slopes. The results indicated that increasing the sand layer thickness increased the initial runoff time, which was consistent with the finding of previous studies (Zhang et al., 1999; Xu et al., 2015). The total runoff yield decreased with the increasing thickness of the sand layer, which was consistent with the results of Zhang et al. (1999) but was inconsistent with those of Xu et al. (2015). The main reason for this inconsistency might be that Xu et al. (2015) used the same duration of runoff production time rather than the same duration of rainfall to calculate the total runoff yield. The variations in initial runoff time and total runoff yield between the uncovered and sand-covered loess slopes resulted from the sharp changes in the hydrophysical properties at the loess soil and aeolian sand interface. Other studies have illustrated that very

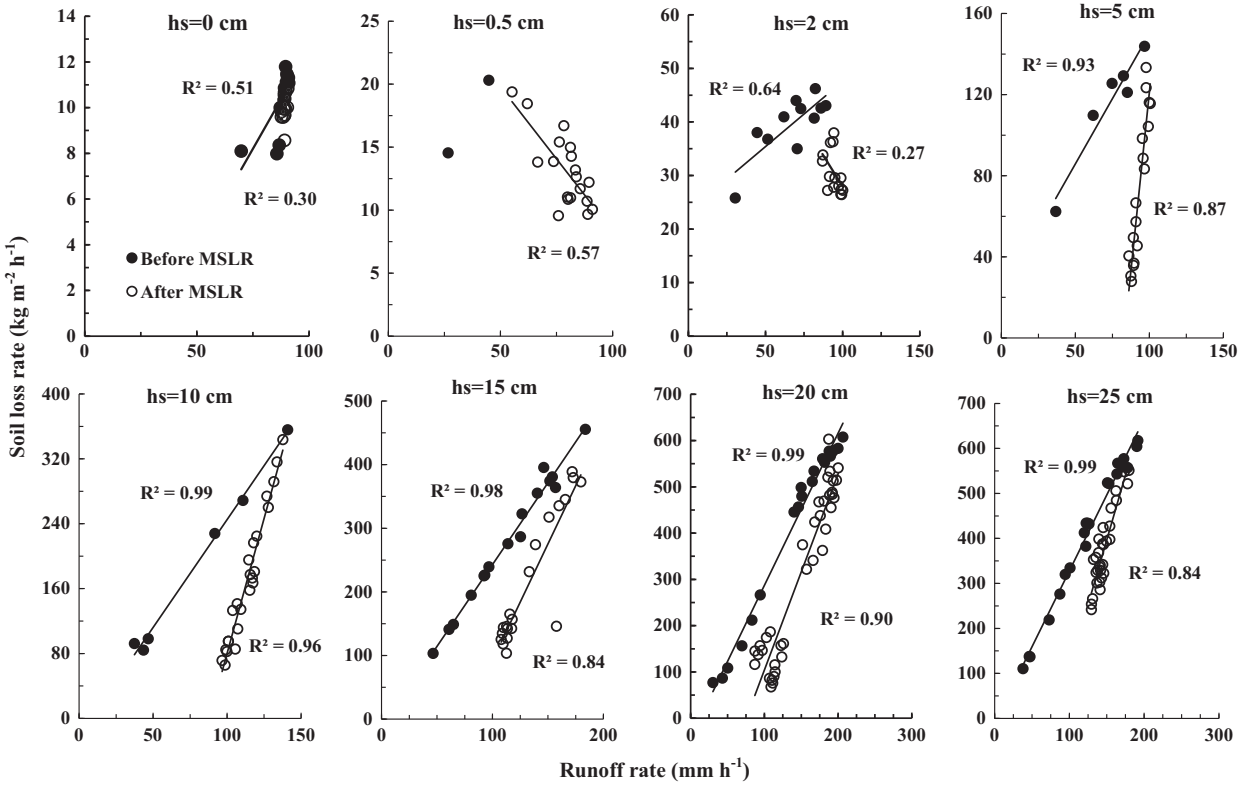

Fig. 3. Relationships between the runoff and soil loss rates on the loess slopes covered with aeolian sand layers of different thicknesses (hs) before and after the maximum soil loss rate (MSLR) during a simulated rainstorm.

different permeabilities of subsoil and surface soil layers had the greatest influence on the hydrological behavior of texture-contrast soils (Cox and McFarlane, 1995; Eastham et al., 2000; Gregory et al., 1992; Hardie et al., 2013). A covering sand layer could change the runoff production mode. Runoff generated on the uncovered loess slope was infiltration excess runoff. In contrast, the runoff produced on the sand-covered loess slopes was mainly subsurface saturation excess runoff or subsurface flow produced at the sand-loess interface due to the sharp change in permeability between top sand layer and underlying loess. This is similar to runoff production on other texture-contrast soil slopes (Eastham et al., 2000; Fox and Wilson, 2010; Hardie et al., 2013). Compared to infiltration excess runoff, subsurface saturation excess runoff or subsurface flow required water to reach a critical water table depth within the sand layer in order to initiate runoff (Dunne, 1990; Iida, 2004; Fox and Wilson, 2010), which increased the initial runoff time. The longer initial runoff time and pressure head of that water table on the loess surface increased the infiltration volume before runoff was produced, which could reduce the total runoff yield. The roughly similar values of the runoff initial time and the total runoff during this stage that occurred with the sand layer thicknesses of 15–25 cm could be expected from the rainfall infiltration theory for sloping surfaces (Chen and Young, 2006) and in stratified media (Chu and Mariño, 2005). The results illustrated that critical hydraulic parameters that trigger runoff and sediment production exist on the aeolian sand-covered loess slopes at a certain sand layer thickness. Previous studies have identified such critical hydraulic parameters, which were expressed in terms of the critical depth of saturated soil, the critical hydraulic gradient and the critical shear stress (Dunne, 1990; Iida, 2004; Fox and Wilson, 2010).

Increasing sand layer thickness could change the runoff production mode that would result in the significant variations observed in runoff rates during the rainstorm. However, the response to variations in runoff rate during the rainfall was different with the various sand layer thicknesses. With a lower water storage capacity, the thinner sand layer treatments (0.5 and 2 cm) were readily saturated by infiltrating rainwater. This water was then exfiltrated at all positions of the slope to produce the overland flow that occurred as saturation excess runoff, which resulted in the roughly similar trends observed in the runoff rates to those of the uncovered loess slope (Fig. 1). This was consistent with the findings of Xu et al. (2015) who also studied sand layer thicknesses ranging from 0 to 1.5 cm over loess. In the cases of the thicker sand layers that had greater water storage capacities, a water table and seepage/subsurface flow were produced within the sand layer and water initially exfiltrated at the toe of the sand layer where the critical hydraulic gradient was first attained (Dunne, 1990; Iida, 2004; Fox and Wilson, 2010). However, once runoff was initiated, runoff rates varied significantly in conjunction with the process of headward erosion that decreased the thickness of the sand layer, reduced confining pressure and released stored rainwater, which resulted in the obviously unimodal distributions of runoff during the rainstorms. In addition, the increasing water holding capacity of the sand layers with increases in thickness and the accelerating headward erosion (Kirkby and Chorley, 1967; Dunne and Black, 1970; Dunne, 1990) resulted in part in runoff coefficients that were greater than 1 and, in some cases, greater than 2. These high runoff coefficients occurred during the rainstorms when the sand layers were more than 2 cm thick, and the maximum runoff coefficient for each of these treatments increased with increases in the sand layer thickness, which is a different result from those of other studies on uniform soil slopes (Martínez-Murillo et al., 2013; Zhao et al., 2013). This result further confirmed that increasing the sand layer thickness could radically change the runoff production processes.

Consistent with previous findings (Zhang et al., 1999; Xu et al., 2015), sediment yields produced on the sand-covered loess slopes were significantly greater than that on the uncovered loess slope. Sediment yield rapidly increased with increasing sand layer thicknesses during the rainstorm. Non-cohesive aeolian sand lacked the capacity to strongly resist the runoff shear stress as compared with the loess soil and consequently supplied ample amounts of erodible material that increased with increasing sand layer thickness. The hydraulic head, soil pore pressure and the interflow water velocity within the sand layer could further reduce the sand layer resistance against the runoff shear stress (Vollmer and Kleinhans, 2007), decrease the Coulomb friction and trigger sand layer failure similar to the landslides described in other studies (Iverson, 2000; Okura et al., 2002; Wang and Sassa, 2003; Lourenço et al., 2006). These factors all led to the rapid increases in sediment yield observed on the sand-covered loess slopes in spite of the longer initial runoff time and reductions in total runoff yield with increasing sand layer thickness.

Increasing sand layer thickness resulted in significant variations in soil loss rates during the rainstorms. The thinner sand layers (0.5 cm and 2 cm) exhibited flow erosion across the entire slope that led to weaker variations in soil loss rate, whereas the thicker sand layers (5 cm–25 cm) exhibited retrogressive sliding from the downslope to the upslope areas that led to stronger variations and obvious unimodal distributions in the soil loss rates as the rainstorms progressed (Fig. 4). These latter effects were also observed in studies of rainfall-induced debris flows or shallow landslide experiments (Okura et al., 2002; Onda et al., 2004; Bogaard and Greco, 2016; Kaitna et al., 2016). These results suggest that increasing sand layer thickness also gradually affected the sediment production mode because there was an increase in the mass of the sand layer that induced an increase in the gravitational driving force along the slope surface (Pornprommin et al., 2010). There were no tension cracks in sand layers that were 5 cm thick or less. However, tension cracks appeared in the sand layers that were 10 cm thick or more (Fig. 4). These observations confirmed the effect of sand layer thickness and the role of the gravity stresses in the sand layer on the failure modes of the sand layer. This finding implies that changes in failure modes might occur in sand layers when the thickness was about 10 cm. Combining the changes in initial runoff time and total runoff yield with increasing sand layer thickness as described above, we speculated that a critical sand layer thickness might exist between 5 cm and 10 cm thick above which a qualitative change in runoff and sediment production patterns could occur, i.e., failures similar to shallow landslides, might occur on the sand-covered loess slopes. This finding may be of great importance to the control and prediction of soil losses in a region with sand-covered loess slopes.

The various sand layer thicknesses changed the relationships between the runoff and soil loss rates on the sand-covered loess slopes during the rainstorms, especially on the loess slopes covered with the thicker sand layers. The variations in the soil loss rates were almost synchronous with those of the runoff rates, and their peak values occurred almost simultaneously during the rainstorms on the loess slopes covered by thicker sand layers. These relationships differed from those obtained for the uncovered loess slope (He et al., 2014; Zhang et al., 2014; Fang et al., 2015). These coinciding variations are ascribed to the effects of sand layer thickness on runoff production and the failure mode of the sand layer as described above. Rainwater stored within the sand layer triggered the sand layer failure, and then the rapid collapse of the sand layer, in turn, facilitated the rapid release of rainwater from the sand layer. These interactions between runoff and sediment production resulted in the positive linear relationship between the runoff and soil loss rates on the sand-covered loess slopes during the rainstorms. The results suggest that although the sand layer can delay

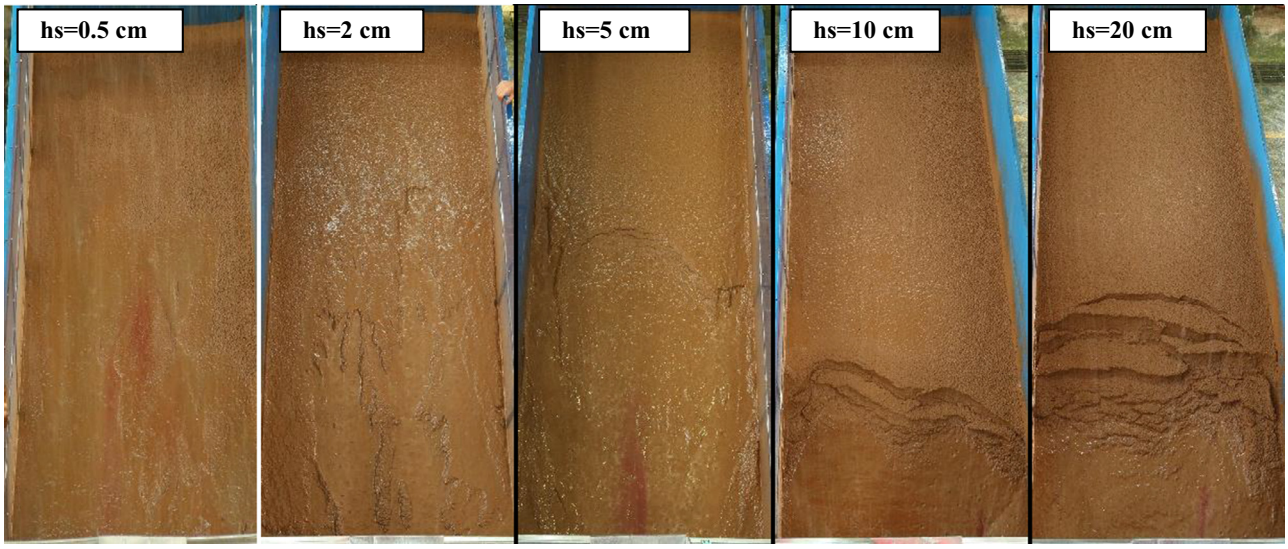

Fig. 4. Examples of failure modes for aeolian sand layers of different thicknesses (hs) overlying loess slopes.

the production of runoff and reduce the total runoff yield, an aeolian sand-covered slope could potentially cause disasters related to landslides and sediment laden floodwater when heavy or prolonged rainfall events occur. The synchronously abrupt increase of runoff and sediment on thicker aeolian sand-covered loess slopes might lead to downstream hazards during the rainstorms.

5. Conclusions

In this study, the runoff and sediment produced on loess slopes covered with aeolian sand layers of different thicknesses were investigated in the laboratory using simulated rainfall. The runoff and soil loss characteristics on the sand-covered loess slopes were notably different from those on the uncovered loess slope and markedly varied with increasing sand layer thickness. Compared with the uncovered loess slope, the sand layers covering the loess slope increased the initial runoff time, reduced the total runoff yield and increased the total sediment yield. The variations in runoff and soil loss rates during the rainfall were enhanced with increasing sand layer thickness. Both rates presented unimodal distributions and varied synchronously during the rainstorms on the loess slopes covered with thicker sand layers. The maximum runoff and soil loss rates during the rainstorm also increased with increasing sand layer thickness and they both had a significant linear positive correlation and largely appeared simultaneously. Interestingly, some runoff coefficients were greater than 1, and even greater than 2 in some cases, on the loess slopes covered with the thicker sand layers during the rainstorms. A critical sand layer thickness that controlled the qualitative changes in runoff and sediment production patterns might exist between 5 and 10 cm thick in this study. The results of this study highlight the important effects of sand thickness on runoff and sediment production on the sand-covered loess slopes. Furthermore, the results imply that geologic hazards might be generated on the sand-covered loess slopes during heavy or prolonged rainfall events and that aeolian sand layer thickness should be considered when assessing and predicting soil losses in this region, especially when considering the downstream impacts on the Yellow River riverbeds.

Acknowledgments

This work was supported by the National Natural Science Foundation of China (41571130082, 41371283, and 41330858) and the National Key Research and Development Program of China (2016YFC0402406). The authors are grateful to Juan V. Giraldez and David Warrington for providing many useful comments and suggestions and for improving the English.

References

Bogaard, T.A., Greco, R., 2016. Landslide hydrology: from hydrology to pore pressure. Wiley Interdiscip. Rev. Water 3, 439–459. http://dx.doi.org/10.1002/wat2.1126.

Chen, L., Young, M.H., 2006. Green-Ampt infiltration model for sloping surfaces. Water Resour. Res. 42. http://dx.doi.org/10.1029/2005WR004468.

Chittleborough, D.J., 1992. Formation and pedology of duplex soils. Aust. J. Exp. Agric. 32, 815–825.

Chu, X., Mariño, M.A., 2005. Determination of ponding condition and infiltration into layered soils under unsteady rainfall. J. Hydrol. 313, 195–207. http://dx.doi.org/10.1016/j.jhydrol.2005.03.002.

Cox, J.W., McFarlane, D.J., 1995. The causes of waterlogging in shallow soils and their drainage in southwestern Australia. J. Hydrol. 167, 175–194. http://dx.doi.org/10.1016/0022-1694(94)02614-H.

Cox, J.W., Chittleborough, D.J., Brown, H.J., Pitman, A., Varcoe, J.C.R., 2002. Seasonal changes in hydrochemistry along a toposequence of texture-contrast soils. Soil Res. 40, 581–604. http://dx.doi.org/10.1071/SR01042.

Dunne, T., 1990. Hydrology, mechanics, and geomorphic implications of erosion by subsurface flow. Spec. Paper-Geol. Soc. Am. 252, 1–28.

Dunne, T., Black, R.D., 1970. An experimental investigation of runoff production in permeable soils. Water Resour. Res. 6, 478–490. http://dx.doi.org/10.1029/WR006i002p00478.

Eastham, J., Gregory, P.J., Williamson, D.R., 2000. A spatial analysis of lateral and vertical fluxes of water associated with a perched watertable in a duplex soil. Soil Res. 38, 879–890. http://dx.doi.org/10.1071/SR99003.

Fang, H., Sun, L., Tang, Z., 2015. Effects of rainfall and slope on runoff, soil erosion and rill development: an experimental study using two loess soils. Hydrol. Process. 29, 2649–2658. http://dx.doi.org/10.1002/hyp.10392.

Fox, G.A., Wilson, G.V., 2010. The role of subsurface flow in hillslope and stream bank erosion: a review. Soil Sci. Soc. Am. J. 74, 717–733. http://dx.doi.org/10.2136/sssaj2009.0319.

Fox, G.A., Wilson, G.V., Simon, A., Langendoen, E.J., Akay, O., Fuchs, J.W., 2007. Measuring streambank erosion due to ground water seepage: correlation to bank pore water pressure, precipitation and stream stage. Earth Surf. Processes Landforms 32, 1558–1573. http://dx.doi.org/10.1002/esp.1490.

Gregory, P.J., Tennant, D., Hamblin, A.P., Eastham, J., 1992. Components of the water balance on duplex soils in western Australia. Rev. Fac. Odontol. Univ. Fed. Bahia 32, 39–55.

Hardie, M.A., Cotching, W.E., Doyle, R.B., Holz, G., Lisson, S., Mattern, K., 2011. Effect of antecedent soil moisture on preferential flow in a texture-contrast soil. J. Hydrol. 398, 191–201. http://dx.doi.org/10.1016/j.jhydrol.2010.12.008.

Hardie, M.A., Doyle, R.B., Cotching, W.E., Lisson, S., 2012a. Subsurface lateral flow in texture-contrast (duplex) soils and catchments with shallow bedrock. Appl. Environ. Soil Sci. 2012, 861358. http://dx.doi.org/10.1155/2012/861358.

Hardie, M.A., Doyle, R.B., Cotching, W.E., Mattern, K., Lisson, S., 2012b. Influence of antecedent soil moisture on hydraulic conductivity in a series of texture-contrast soils. Hydrol. Process. 26, 3079–3091. http://dx.doi.org/10.1002/hyp.8325.

Hardie, M.A., Doyle, R., Cotching, W., Holz, G., Lisson, S., 2013. Hydropedology and preferential flow in the tasmanian texture-contrast soils. Vadose Zone J. 12. http://dx.doi.org/10.2136/vzj2013.03.0051.

He, J., Li, X., Jia, L., Gong, H., Cai, Q., 2014. Experimental study of rill evolution processes and relationships between runoff and erosion on clay loam and loess. Soil Sci. Soc. Am. J. 78, 1716–1725. http://dx.doi.org/10.2136/sssaj2014.02.0063.

Iida, T., 2004. Theoretical research on the relationship between return period of rainfall and shallow landslides. Hydrol. Process. 18, 739–756. http://dx.doi.org/10.1002/hyp.1264.

Iverson, R.M., 2000. Landslide triggering by rain infiltration. Water Resour. Res. 36, 1897–1910. http://dx.doi.org/10.1029/2000WR900090.

Kaitna, R., Palucis, M.C., Yohannes, B., Hill, K.M., Dietrich, W.E., 2016. Effects of coarse grain size distribution and fine particle content on pore fluid pressure and shear behavior in experimental debris flows. J. Geophys. Res. 121, 415–441. http://dx.doi.org/10.1002/2015JF003725.

Karmaker, T., Dutta, S., 2013. Modeling seepage erosion and bank retreat in a composite river bank. J. Hydrol. 476, 178–187. http://dx.doi.org/10.1016/j.jhydrol.2012.10.032.

Kim, M.S., Onda, Y., Kim, J.K., Kim, S.W., 2015. Effect of topography and soil parameterisation representing soil thicknesses on shallow landslide modelling. Quat. Int. 384, 91–106. http://dx.doi.org/10.1016/j.quaint.2015.03.057.

Kirkby, M., Chorley, R., 1967. Throughflow, overland flow and erosion. Hydrol. Sci. J. 12, 5–21. http://dx.doi.org/10.1080/02626667709493533.

Lanni, C., McDonnell, J., Hopp, L., Rigon, R., 2013. Simulated effect of soil depth and bedrock topography on near-surface hydrologic response and slope stability. Earth Surf. Processes Landforms 38, 146–159. http://dx.doi.org/10.1002/esp.3267.

Li, M., Li, Z.-B., Liu, P.-L., Yao, W.-Y., 2005. Using Cesium-137 technique to study the characteristics of different aspect of soil erosion in the wind-water erosion crisscross region on Loess Plateau of China. Appl. Radiat. Isot. 62, 109–113. http://dx.doi.org/10.1016/j.apradiso.2004.06.005.

Lourenço, S.D.N., Sassa, K., Fukuoka, H., 2006. Failure process and hydrologic response of a two layer physical model: implications for rainfall-induced landslides. Geomorphology 73, 115–130. http://dx.doi.org/10.1016/j.geomorph.2005.06.004.

Martínez-Murillo, J.F., Nadal-Romero, E., Regüés, D., Cerdà, A., Poesen, J., 2013. Soil erosion and hydrology of the western Mediterranean badlands throughout rainfall simulation experiments: a review. Catena 106, 101–112. http://dx.doi.org/10.1016/j.catena.2012.06.001.

Northcote, K.H., 1971. A Factual Key for the Recognition of Australian Soils. Rellim Technical Publications, Australia.

Okura, Y., Kitahara, H., Ochiai, H., Sammori, T., Kawanami, A., 2002. Landslide fluidization process by flume experiments. Eng. Geol. 66, 65–78. http://dx.doi.org/10.1016/S0013-7952(02)00032-7.

Onda, Y., Tsujimura, M., Tabuchi, H., 2004. The role of subsurface water flow paths on hillslope hydrological processes, landslides and landform development in steep mountains of Japan. Hydrol. Process. 18, 637–650. http://dx.doi.org/10.1002/hyp.1362.

Pornprommin, A., Takei, Y., Wubneh, A.M., Izumi, N., 2010. Channel inception in cohesionless sediment by seepage erosion. J. Hydro-Environ. Res. 3, 232–238. http://dx.doi.org/10.1016/j.jher.2009.10.011.

Rab, M., Willatt, S., Olsson, K., 1987. Hydraulic properties of a duplex soil determined from in situ measurements. Soil Res. 25, 1–7. http://dx.doi.org/10.1071/SR9870001.

Raj, M., Sengupta, A., 2014. Rain-triggered slope failure of the railway embankment at Malda, India. Acta Geotech. 9, 789–798. http://dx.doi.org/10.1007/s11440-014-0345-9.

Tang, K.L., 1990. Regional Characteristics of Soil Erosion and its Control Approaches on Loess Plateau (in Chinese). Science Press, Beijing.

Tennant, D., Scholz, G., Dixon, J., Purdie, B., 1992. Physical and chemical characteristics of duplex soils and their distribution in the south-west of western Australia. Aust. J. Exp. Agric. 32, 827–843. http://dx.doi.org/10.1071/EA9920827.

Vollmer, S., Kleinhans, M.G., 2007. Predicting incipient motion, including the effect of turbulent pressure fluctuations in the bed. Water Resour. Res. 43, 297–304. http://dx.doi.org/10.1029/2006WR004919.

Wang, G., Sassa, K., 2003. Pore-pressure generation and movement of rainfall-induced landslides: effects of grain size and fine-particle content. Eng. Geol. 69, 109–125. http://dx.doi.org/10.1016/S0013-7952(02)00268-5.

Wang, L., Mu, Y., Zhang, Q.F., Jia, Z.K., 2012. Effects of vegetation restoration on soil physical properties in the wind-water erosion region of the northern Loess Plateau of China. Clean-Soil Air Water 40, 7–15. http://dx.doi.org/10.1002/clen.201100367.

Wu, X., Zhang, F., Wang, Z., 2014. Variation of sand and loess properties of binary structure profile in hilly region covered by sand of the Loess Plateau. J. Soil Water Conserv. 29, 190–193 (in Chinese with English abstract).

Xu, J.X., 2000. The wind-water two-phase erosion and sediment-producing processes in the middle Yellow River basin, China. Sci. China Ser. D Earth Sci. 43, 176–186. http://dx.doi.org/10.1007/bf02878147.

Xu, J.X., 2005a. Hyperconcentrated flows as influenced by coupled wind-water processes. Sci. China Ser. D Earth Sci. 48, 1990–2000. http://dx.doi.org/10.1360/04yd0307.

Xu, J.X., 2005b. Influences of coupled wind-water processes on suspended sediment grain size: an example from tributaries of the Yellow River. Hydrol. Sci. J. 50, 881–895. http://dx.doi.org/10.1623/hysj.2005.50.5.881.

Xu, J., Lu, G., Gan, Z., 2000. Definition of coarse silt and silty area in the middle reach of the Yellow River. China Water Resour. 12, 37–38 (in Chinese with English abstract).

Xu, J.X., Yang, J.S., Yan, Y.X., 2006. Erosion and sediment yields as influenced by coupled eolian and fluvial processes: the Yellow River, China. Geomorphology 73, 1–15. http://dx.doi.org/10.1016/j.geomorph.2005.03.012.

Xu, G.C., Tang, S.S., Lu, K.X., Li, P., Li, Z.B., Gao, H.D., Zhao, B.H., 2015. Runoff and sediment yield under simulated rainfall on sand-covered slopes in a region subject to wind-water erosion. Environ. Earth Sci. 74, 2523–2530. http://dx.doi.org/10.1007/s12665-015-4266-1.

Zeng, L., Fu, H.Y., Li, T., Qin, Y.Q., 2012. The analysis of seepage characteristics and stability of carbonaceous mudstone embankment slope in rainfall condition. Adv. Mat. Res. 446–449, 1864–1868. http://dx.doi.org/10.4028/www.scientific.net/AMR.446-449.1864.

Zhang, L., Tang, K., Zhang, P., 1999. Soil water erosion processes in loess hilly-gully region covered with sheet sand. J. Soil Eros. Soil Water Conserv. 5, 40–45 (in Chinese with English abstract).

Zhang, F.-B., Wang, Z.-L., Yang, M.-Y., 2014. Validating and improving interrill erosion equations. PLoS One 9, e88275. http://dx.doi.org/10.1371/journal.pone.0088275.

Zhao, X., Wu, P., Chen, X., Helmers, M.J., Zhou, X., 2013. Runoff and sediment yield under simulated rainfall on hillslopes in the Loess Plateau of China. Soil Res. 51, 50–58. http://dx.doi.org/10.1071/SR12239.

Zhou, J.J., Zhang, M., 2012. Coarse sediment and lower Yellow River siltation. J. Hydro-Environ. Res. 6, 267–273. http://dx.doi.org/10.1016/j.jher.2012.05.005.